Supplementary Information Appendix for:

Atomic-level mechanisms for phospholamban regulation of the calcium pump

L. Michel Espinoza-Fonseca[1], Joseph M. Autry[1], G. Lizbeth Ramírez-Salinas[2], and David D. Thomas[1]

[1]Department of Biochemistry, Molecular Biology and Biophysics, University of Minnesota, Minneapolis, MN 55455

[2]Laboratorio de Modelado Molecular y Bioinformática, Escuela Superior de Medicina, Instituto Politécnico Nacional, Mexico City 11340, Mexico

This file includes:

Construction of the SERCA-PLB complex

The structure of the cytoplasmic domain of PLB was modeled using the NMR ensemble of rabbit PLB in its monomeric form (PDB: 2kb7) (1). The amino acid sequences of rabbit PLB and PLB4 are shown in (**Figure S2**). We used several criteria to select the most appropriate conformation to construct the full structure of PLB in the complex because NMR spectroscopy resolved multiple orientations of the cytoplasmic domain of PLB. First, we superimposed residues 24-49 of each structure in the 20-structure NMR ensemble on residues 23-48 of PLB4 in the crystal structure. Upon alignment, we discarded unrealistic structures of PLB, i.e., structure where the cytoplasmic domain of PLB is inserted in the structure of SERCA. Only 15 of the 20 NMR structures were considered as potential templates to model the structure of full-length PLB (**Figure S10**). Next, we used the PPM server (2) to determine the position of the crystal structure of SERCA-PLB4 in a lipid bilayer. We selected only structures of PLB where the cytoplasmic domain is perpendicular to the bilayer normal and discarded structures where the cytoplasmic domain is embedded in the lipid bilayer (i.e., structures NMR-1, NMR-4 and NMR-5, (**Figure S10**). This filtering procedure yielded 7 potential templates: structures NMR-2, NMR-3, NMR-9, NMR-14, NMR-15, NMR-16 and NMR-19 (**Figure S10**). Based on the structural identity of these structures, the seven conformations were clustered in two conformations: conformation NMR-A, represented by the average structure of NMR-2, NMR-3, NMR-9, NMR-15, NMR-16 and NMR-19, and NMR-B, represented by structure NMR-14 (**Figure S10**).

We used structures NMR-A and NMR-B to obtain the best possible model of full-length PLB in the complex. Modeling was done by fusing residues 1-20 of NMR-A and

NMR-B to residues 21-48 of PLB in the crystal structure. The structure NMR-B was used to reconstruct the C-terminus of PLB (residues M50-L52). Finally, residues A27, C30, A37 and G49 of PLB4 were changed to N27, N30, L37 and V49 to produce a model of rabbit PLB. The stereochemical quality of the initial models was verified with PROCHECK (3, 4), showing no major aberrations in the geometry of the complexes. We performed several 20-ns MD simulations of the fully solvated SERCA-PLB complex starting from the conformations NMR-A and NMR-B of PLB. MD simulations showed that in all cases, conformation NMR-A converges toward NMR-B, but MD simulations starting from NMR-B do not converge toward NMR-A (**Figure S11**). This indicates that NMR-B represents a relaxed structure of PLB in the complex. Therefore, we used NMR-B [model 14 of the NMR ensemble of rabbit AFA-PLB mutant (1)] as the starting conformation to simulate the dynamics of SERCA-PLB.

Table S1. SERCA crystal structures used for MD and structural analyses. PDB codes, bound ligands, and biochemical state assignments are indicated.

Cation-bound crystal structures

PDB ID	Ligands in crystal	Assigned biochemical state
1su4	$2Ca^{2+}$	E1•$2Ca^{2+}$
1vfp	$2Ca^{2+}$, AMPPCP	E1•$2Ca^{2+}$•ATP
1t5s	$2Ca^{2+}$, AMPPCP	E1•$2Ca^{2+}$•ATP
3ar2	$2Ca^{2+}$, AMPPCP	E1•$2Ca^{2+}$•ATP
3n8g	$2Ca^{2+}$, AMPPCP	E1•$2Ca^{2+}$•ATP
3w5a	Mg^{2+}, Sarcolipin	E1•Mg^{2+}-SLN
3w5b	Mg^{2+}	E1•Mg^{2+}
4h1w	$2Mg^{2+}$, Sarcolipin	E1•$2Mg^{2+}$-SLN

Cation-free crystal structures

PDB ID	Ligands in crystal	Assigned biochemical state
1iwo	Thapsigargin	E2•$3H^+$
2agv	Thapsigargin, BHQ	E2•$3H^+$
2ear	Thapsigargin	E2•$3H^+$
2eat	Thapsigargin, Cyclopiazonic acid	E2•$3H^+$
2c8k	Thapsigargin, AMPPCP	E2•$3H^+$•ATP
2eau	Cyclopiazonic acid	E2•$3H^+$
3w5c	-	E2•$3H^+$
4kyt	Phospholamban	[a]E2•$3H^+$ // [b]E1•$H_{771}{}^+$

[a]Akin et al. (5)
[b]This study.

Table S2. Predicted pK_a values of acidic residues using different crystal structures of SERCA.

	Cation-bound crystal structures (E1)			
PDB code	**E309**	**E771**	**D800**	**E908**
1su4	10.5	3.3	-0.5	8.8
1vfp	6.1	2.7	0.1	8.7
3w5a	5.6	6.6	2.9	8.8
3w5b	6.7	5.3	3.5	9.7
3AR2	6.1	1.0	2.6	8.9
1t5s	6.6	2.6	-0.2	9.0
4h1w	-0.2	6.2	2.8	8.0
3n8g	5.8	3.2	-0.2	8.5
	Cation-free crystal structures (E2)			
PDB code				
1iwo	6.4	10.8	6.8	10.1
2agv	8.7	10.9	8.2	9.7
2ear	8.3	10.5	8.0	9.9
2eat	8.7	10.3	7.0	11.6
2c8k	9.0	10.5	7.8	10.0
3w5c	9.7	11.1	7.3	9.4
2eau	9.7	10.8	7.2	9.6

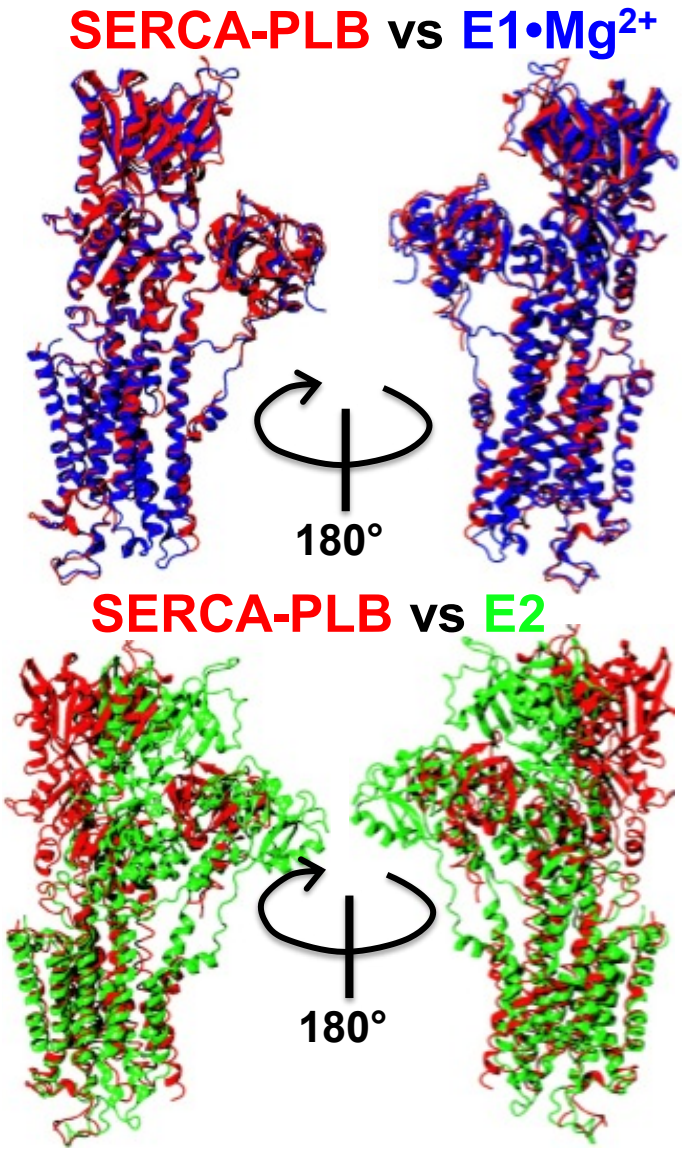

Figure S1. Comparison between SERCA-PLB, E2 and E1 SERCA. The TM domain of SERCA-PLB (red ribbons) were superposed with E1.Mg2+ (blue, PDB: 3w5b) and E2 (green; PDB: 3w5c).

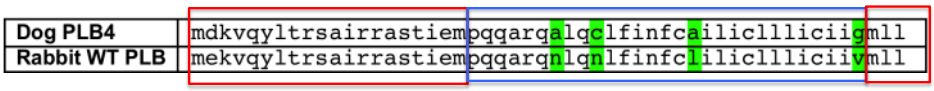

Figure S2. Amino acid sequence of dog mutant PLB4 and rabbit wild-type PLB. The *blue box* indicates the segment of PLB4 that is detected in the x-ray density map of the SERCA-PLB4 complex; the *red boxes* indicate segments of PLB4 that are not detected. Mutations in PLB4 are shaded in *green*.

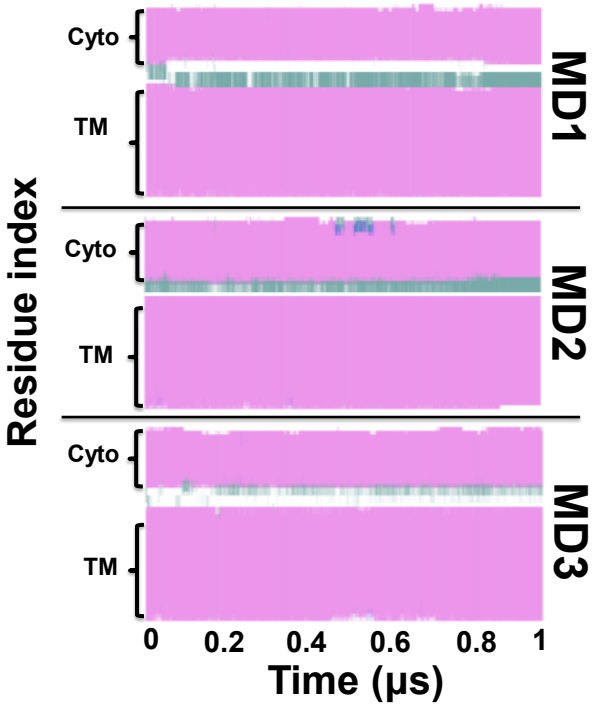

Figure S3. Secondary structure evolution of PLB bound to SERCA. Secondary structure is colored as helix (pink), turn (cyan), and coil (white).The location of the cytoplasmic (residues E2-S16) and TM (residues A24-L51) helices is shown in brackets (left). MD1-MD3 are independent trajectories of the complex.

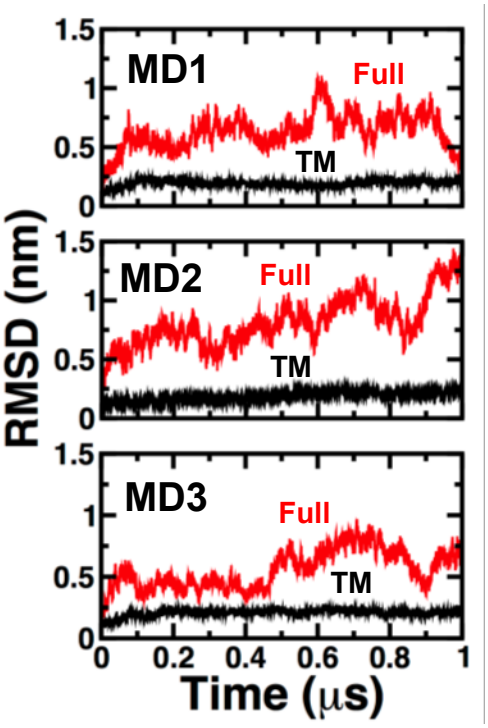

Figure S4. RMSD evolution of PLB bound to SERCA. RMSD was calculated for full-length PLB (red) and TM domain (black). Backbone alignment was used for RMSD calculation of the TM helix. MD1-MD3 are independent trajectories of the complex.

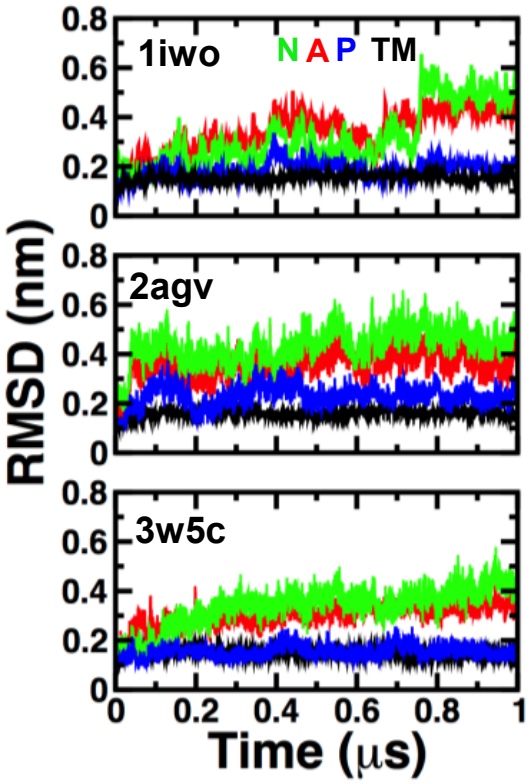

Figure S5. RMSD evolution of E2 domains. RMSD of the TM domain of SERCA was calculated using backbone alignment for TM helices of the pump. RMSD of N, P and A domains was calculated by aligning the backbone of the cytosolic headpiece with the structure at the beginning of each trajectory. The PDB codes (*upper left*) indicate the structures used to generate each trajectory of E2.

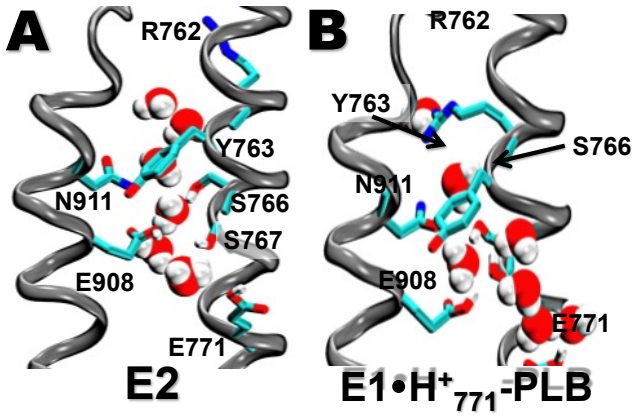

Figure S6. Identification of a water wire in the C-path of SERCA in E2, but not SERCA-PLB inE1•H^+_{771}. (A) Depiction of a water wire in E2. This water wire (6 water molecules) starts in the transport sites and continues along an open C-path delineated by residues Y763, S766, S767 and N911. Residue R762 points away from the path in an "open" position that allows water exchange between the transport sites and the cytosol. (B) The C-path of E1•H^+_{771} is filled with two water molecules around residue N911, but a water wire characteristic of E2 is completely absent. In addition, residue R762 is found in a "closed" position, blocking water access from the cytosol to the Ca^{2+} sites, and vice versa. SERCA is shown as *grey ribbons*, protein side chains as *sticks,* and water molecules *as van der Waals spheres*.

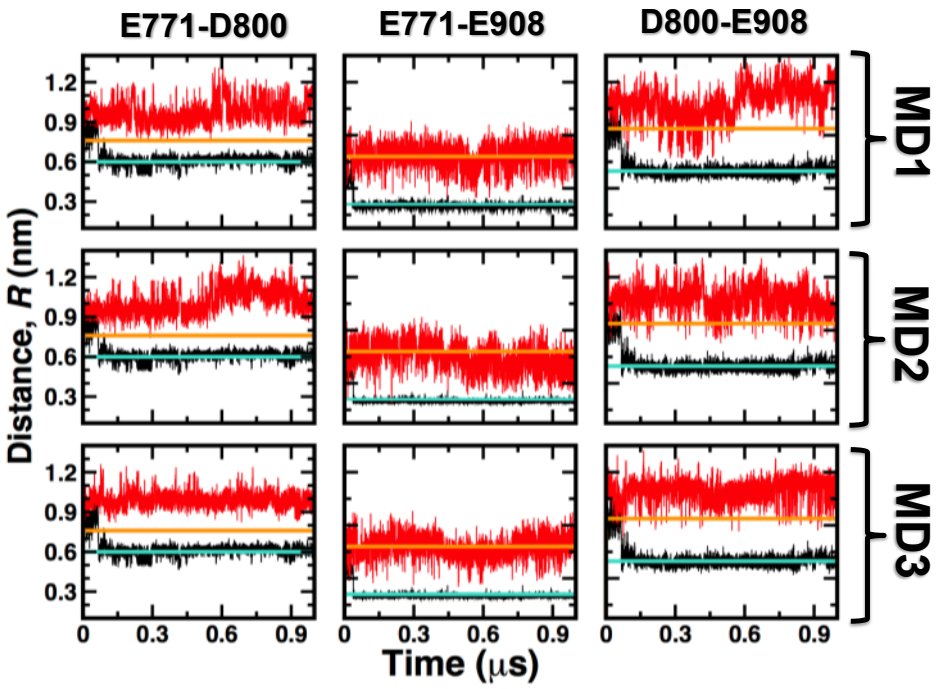

Figure S7. Distance evolution of carboxyl-carboxyl pairs between SERCA residues E771, D800, and E908 in E1•2K$^+$ and E1•H$^+_{771}$. Distances between E771 and D800, were calculated using atoms C_δ and C_γ, respectively. The distance between E771 and E908 (E771-E908) was calculated between the protonated oxygen ($O_{\varepsilon 2}$) from the carboxylic group of E908 and the atom $O_{\varepsilon 1}$ from E771. Finally, the distance D800-E908 was calculated between atoms $O_{\varepsilon 1}$ and C_γ of E908 and D800, respectively. Distances were calculated for MD simulations of E1•H$^+_{771}$ -PLB (red) and compared with E1•2K$^+$ (black). We also show the distances in the crystal structure of SERCA-PLB (4kyt in orange) and E1•2Ca^{2+} (average of 1su4 and 1vfp in cyan). The distances show that E1•H$^+_{771}$ -PLB does not produce a competent transport site I.

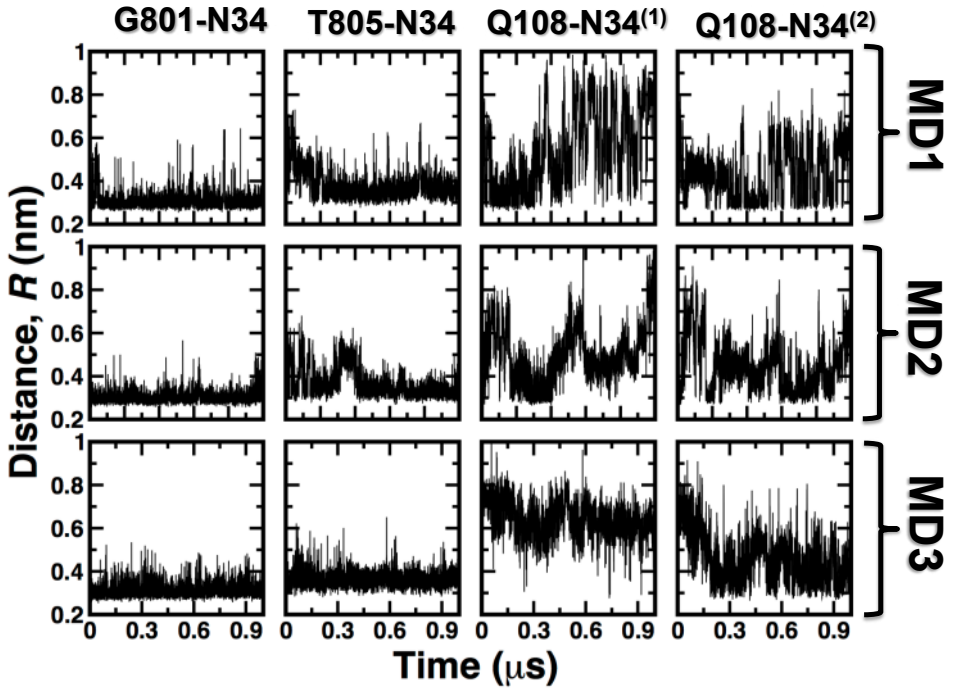

Figure S8. Distance evolution between residues N34 of PLB and Q108, G801 and T805 of E1•H^+_{771}. The plots show that N34 of PLB interacts with G801 and T805 throughout the entire simulation time in all trajectories. Distances between G801 and N34 (G801-N34), were calculated using atoms $O_{backbone}$ and N_δ, respectively. The distance between T805 and N34 (E771-E908) was calculated between the O_γ of T805 and N_δ of N34. The distances Q108-N34$^{(1)}$ and Q108-N34$^{(2)}$ were calculated for O_ε-N_δ and N_ε-O_δ pairs, respectively.

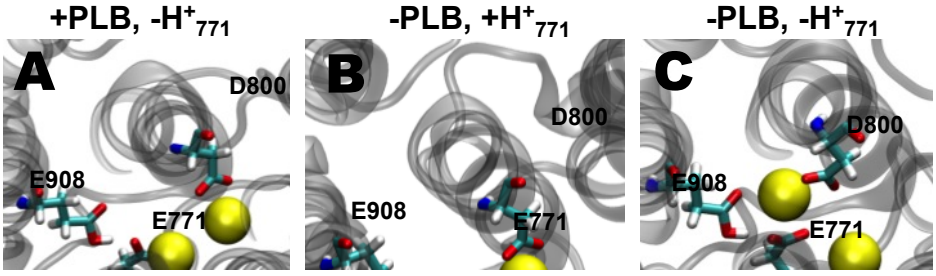

Figure S9. K^+ interactions with SERCA in the transport sites. (A) Structure of the transport sites at the end of the 0.3 μs trajectory of SERCA-PLB with ionized residue E771. (B) Geometry of the transport sites at the end of the MD simulation of apo SERCA in the absence of PLB but protonated on E771. (C) Structure of the transport sites at the end of the 0.3 μs MD simulation of apo SERCA and in the absence of protonation on E771. In all panels, the TM helices are represented by grey ribbons and cation-binding residues are shown as sticks, and K^+ ions are shown as yellow spheres.

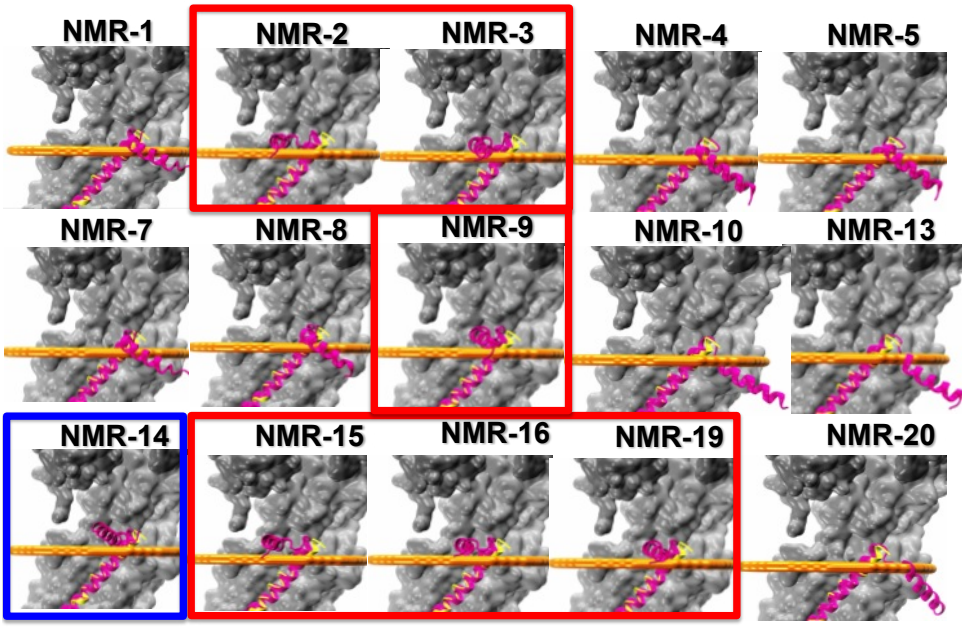

Figure S10. Superposition of NMR structure of PLB on the crystal structure of SERCA-PLB. We show fifteen structures of AFA-PLB considered as potential templates to model the structure of full-length PLB. The structures are labeled using the notation NMR-*X*, where *X* indicates the structure of PLB in the original NMR ensemble (PDB: 2kb7). As described in the Methods section, we found that seven out of fifteen structures were further considered as viable templates to model PLB in the complex. Based on the structural identity of these structures, the seven conformations were clustered in two conformations: conformation NMR-A, represented by the average structure of NMR-2, NMR-3, NMR-9, NMR-15, NMR-16 and NMR-19 (red boxes), and NMR-B, represented by structure NMR-14 (blue box). SERCA is shown as grey surface and PLB4 as yellow ribbons. The NMR structures of PLB are shown as magenta ribbons. The boundaries of the lipid bilayer are shown in orange.

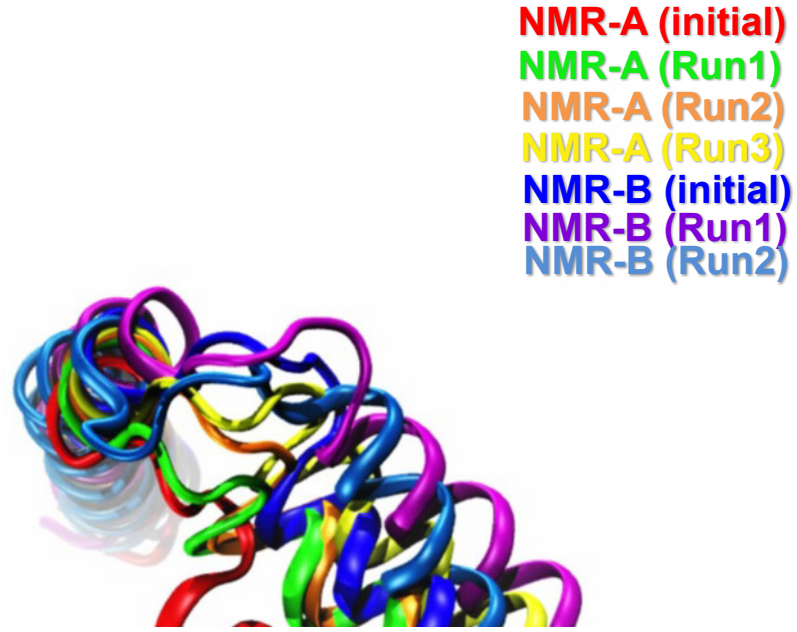

Figure S11. Structural superposition of conformations of structures NMR-A and NMR-B. We show initial and structures at the end of the 20-ns MD simulations. All structures were aligned using residues 23-52.

Supporting References

1. Traaseth, N. J., L. Shi, R. Verardi, D. G. Mullen, G. Barany, and G. Veglia. 2009. Structure and topology of monomeric phospholamban in lipid membranes determined by a hybrid solution and solid-state NMR approach. Proceedings of the National Academy of Sciences of the United States of America 106:10165-10170.
2. Lomize, M. A., I. D. Pogozheva, H. Joo, H. I. Mosberg, and A. L. Lomize. 2012. OPM database and PPM web server: resources for positioning of proteins in membranes. Nucleic acids research 40:D370-376.
3. Laskowski, R. A., M. W. MacArthur, D. S. Moss, and J. M. Thornton. 1993. PROCHECK - a program to check the stereochemical quality of protein structures. J. App. Cryst. 26:283-291.
4. Laskowski, R. A., J. A. Rullmannn, M. W. MacArthur, R. Kaptein, and J. M. Thornton. 1996. AQUA and PROCHECK-NMR: programs for checking the quality of protein structures solved by NMR. Journal of biomolecular NMR 8:477-486.
5. Akin, B. L., T. D. Hurley, Z. Chen, and L. R. Jones. 2013. The structural basis for phospholamban inhibition of the calcium pump in sarcoplasmic reticulum. The Journal of biological chemistry 288:30181-30191.